Electronic supplementary materials *Mendeleev Commun.*, 2020, **30**, 465-467

Nickel-containing nanophases as the carriers of catalytic active sites in the ethylene oligomerization in the presence of systems based on Ni(acac)$_2$ and organoaluminum compounds

Yuliya Y. Titova, Tatyana V. Kon’kova, Boris G. Sukhov and Fedor K. Schmidt

TABLE OF CONTENTS

Experimental Section

General Procedures

Argon (purity at least of 99.999%) was purified from moisture and oxygen by consecutive passing through the columns filled with P_2O_5, granulated alkali, molecular sieves CaA, and powder copper heated at 200 °C. Ethylene (GOST (State Standard) 25070-87, OAO Nizhnekamskneftekhim, purity at least of 99.99%) was used without any pretreatment. Toluene was purified according to the standard protocols applied for handling with organometallic compounds.[S1] To reach a deeper drying, benzene and toluene were additionally distilled over $LiAlH_4$ on the rectifying column and stored under argon in sealed ampoules over molecular sieves 4 Å.

Concentration of water in the solvents, measured by Fischer method,[S2] was about ~1.8 mmol dm^{-3}. The organoaluminum compounds (Et_2AlCl and $Et_2AlCl\cdot Cl_2AlEt$) (Sigma-Aldrich, CAS Number 96-10-6 and CAS Number 12075-68-2) were purified by standard techniques.[S3,S4] Toluene solutions of these organoaluminum compounds were stored in sealed ampoules under argon atmosphere. Nickel bis(acetylacetonate) samples were synthesized by the methods described earlier.[S5] The content of water in the nickel bis(acetylacetonate) samples was determined by simultaneous thermogravimetry–differential scanning calorimetry on a Netzsch Jupiter STA 449 F3 derivatograph (Germany) at a nitrogen flow rate of 30 ml min^{-1} and a heating rate of 5 deg min^{-1}. All manipulations with oxygen- and/or moisture-sensitive materials were performed under an atmosphere of dry argon using standard Schlenk or dry box techniques.

General procedure of the catalyst formation in the presence of ethylene and conducting experiments combining measurement of the rate of ethylene oligomerization.

A 'duck' type reaction vessel was placed on a shaker, connected with a volumetric flask, evacuated twice, and filled with ethylene. The reaction vessel was sequentially loaded with a nickel complex (0.75×10^{-5}–1×10^{-4} mol) and toluene (18–20 ml) as a solvent in an ethylene flow. The reaction mixture was saturated with ethylene by shaking the vessel; thereupon, a cocatalyst solution in toluene was added. The [cocatalyst]/[Ni] ratio was 50. The overall volume of the reaction system was 20 ml. Oligomerization was performed under continuous supply of the reaction vessel with ethylene under pressure of 1 atm and vigorous shaking. The ethylene flow rate was determined volumetrically from the change in the level of decane in the volumetric flask in millimeters (flask volume = 500 ml).

The solutions of the samples were transferred to 4mm vials by the Schlenk method,[S6] which prevented their contact with air. An aliquot of the solution for the preparation of samples for TEM was prepared by the same way. These solutions were diluted with toluene to one-fifth of their original concentration. A drop of the diluted solution was applied to a carbonized copper grid (200 mesh) and dried in a glovebox at ambient temperature under an inert atmosphere.[S5]

Ethylene conversion products were analyzed on a Chromatech-Crystall 5000.2 chromatograph (Chromatech, Russia) equipped with a flame ionization detector using a capillary column (length, 30 m; diameter, 0.53 mm; SGE BPX5 phase) and on a Shimadzu GCMS-QP-2010 mass spectrometer (Japan).[S5] The products of ethylene conversion in the presence of a both catalytic system were generally presented by dimers, trimers, and a small number of oligomers, as namely, butenes (not more than 54–58 %), methylpentenes (20–24 %), linear hexenes (9.5–12.5 %), and oligomers (6.5–9.7 %).

Research methods

ESR-spectroscopy.

EPR spectra were recorded on a ESP 70-03 XD/2 spectrometer (the Experimental Design Office of Special Equipment of Belarus State University, Republic of Belarus) with a working frequency of 9.3 GHz. The spectrometer’s sweep ranges were calibrated using diphenylpicrylhydrazyl of the *N*,*N*-diphenyl-*N′*-picrylhydrazyl radical (DPPH). The model EPR spectra were calculated on a GPU-Tesla computer cluster using the EasySpin module for the MatLab software suite,[S7] taking into account only the Zeeman electron and the hyperfine interaction in the first order of approximation. The concentration of the spins was calculated by comparison with the reference sample representing a $Cu(acac)_2$ solution. Namely, the areas of the ESR signals assigned to Ni^I and Ni^0 were compared with those of the signals of $Cu(acac)_2$ solutions of a certain concentration. All the compared signals were obtained under strictly identical conditions for ESR survey.[S8,S9] To determine the area under the absorption line double integration of spectral curve intensities of the dependence of the first derivative on the field voltage was employed. The integration was carried out using the intrinsic function of mathematical processing of the spectra with a help of a program supplied by the manufacturer of the ESP 70-03 XD/2 instrument.

Transmission electron microscopy.

Images of high resolution transmission electronic microscopy (HRTEM) were obtained on Tecnai G^2 (FEI, USA) electronic microscope with accelerating voltage of 200 kV. The images were recorded using the CCD camera (Soft Imaging System, Germany). Samples were then subjected to chemical microanalysis and annular dark-field imaging. Local elemental analysis was performed with EDX method on Energy-dispersive X-ray Phoenix Spectrometer equipped with Si (Li) detector with energy resolution about 130 eV. Parameters of the particle images were measured using iTEM 5.0 and DigitalMicrographs 1.94.1613 programs. Periodic structures and images filtration were analyzed by the Fourier's method: FFT (Fast Fourier Transformation) and IFFT (Inverse Fast Fourier Transformation). Interlayer distances were determined using profiles of the image intensity obtained by the DigitalMicrographs 3.01.598.0 program. The data obtained by electron diffraction were processed using DiffTools DigitalMicrographs 3.3.1[S10,S11] and OriginPro 8 program package (for baseline correction).[S12]

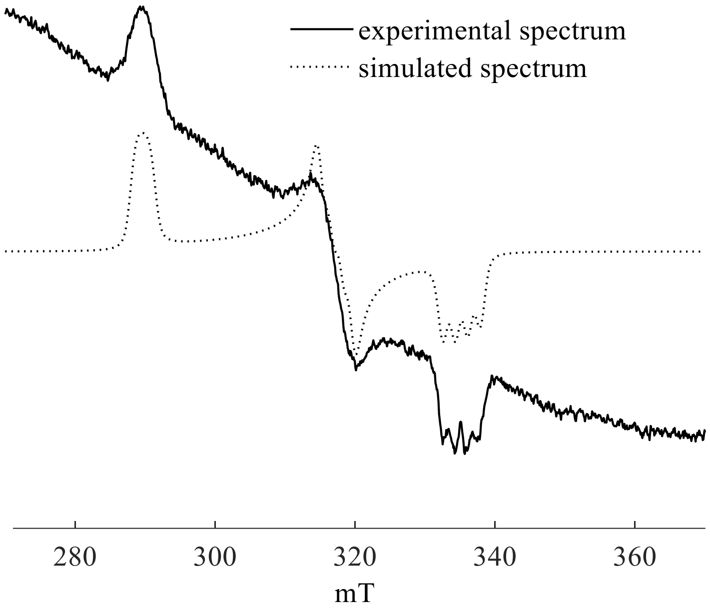

Spectrum data: $g_1 = 2.003$, $g_2 = 2.116$, and $g_3 = 2.318$.

Figure S1 EPR spectrum of toluene solution of Ni(acac)$_2$–DEAC* (0.5 min after mixing the components) reaction mixture in ethylene conversion process (solid line) and model EPR spectrum of Ni(acac)$_2$–DEAC system (dashed line).

*EPR spectrum of toluene solution of Ni(acac)$_2$–EASC system was similar.

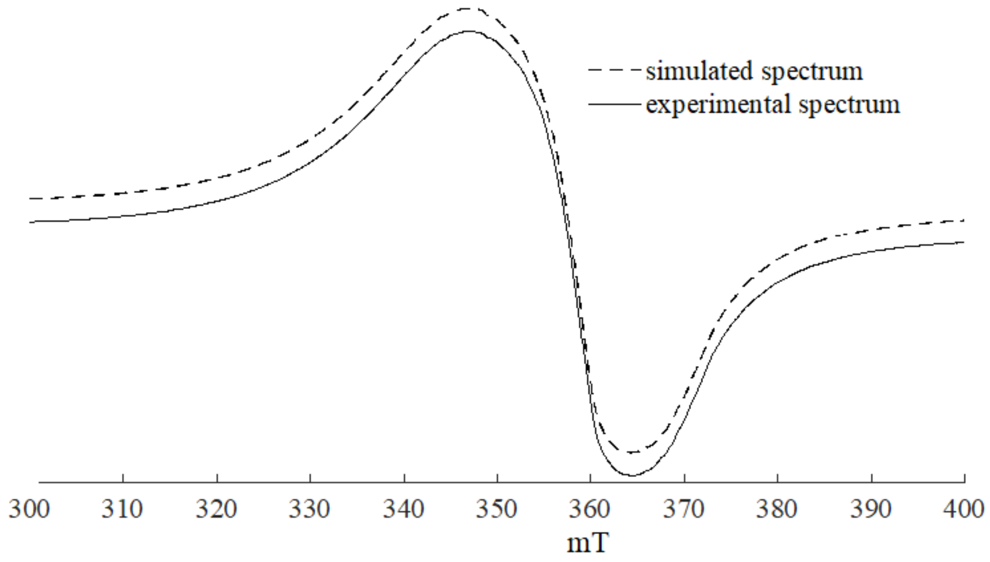

Figure S2 EPR spectrum of toluene solution of $Ni(acac)_2$–DEAC* (4.0 min after mixing the components) reaction mixture in ethylene conversion process (solid line) and model EPR spectrum of $Ni(acac)_2$–50DEAC system (dashed line).

*EPR spectrum of toluene solution of $Ni(acac)_2$–EASC system was similar.

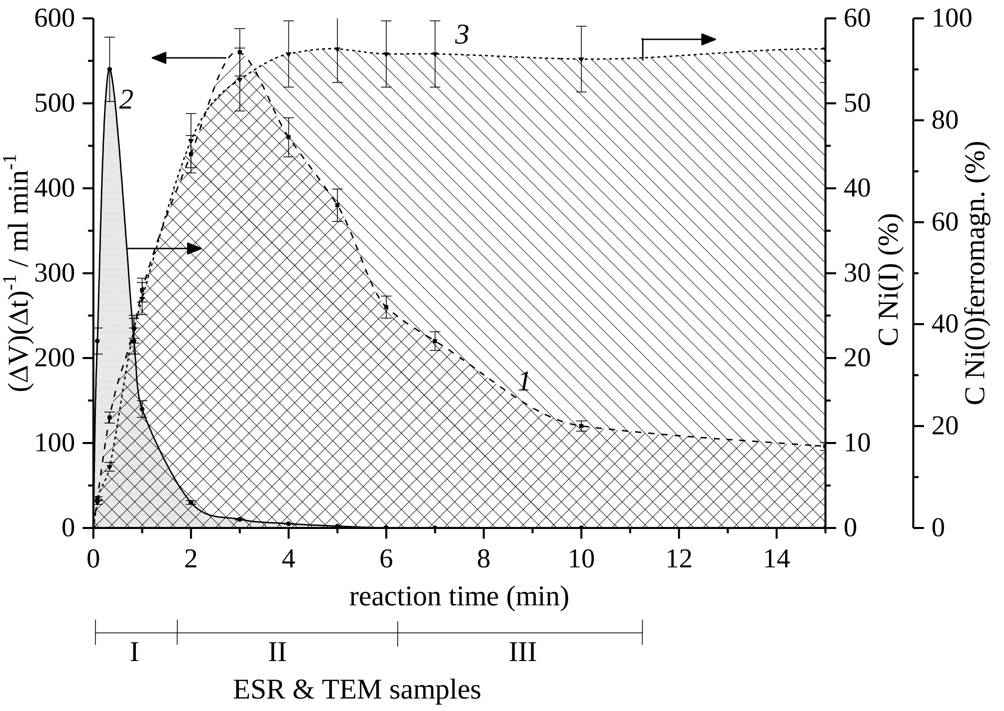

Figure S3 Time dependences of (*1*) ethylene oligomerization rate, (*2*) Ni^I calculated concentration and (*3*) concentration of nickel in the ferromagnetic state for $Ni(acac)_2$–EASC system*. For clarity, data are presented only for first 15 min of experiment.

* See Figure 1 in the main part of the manuscript for these dependences for $Ni(acac)_2$–DEAC system.

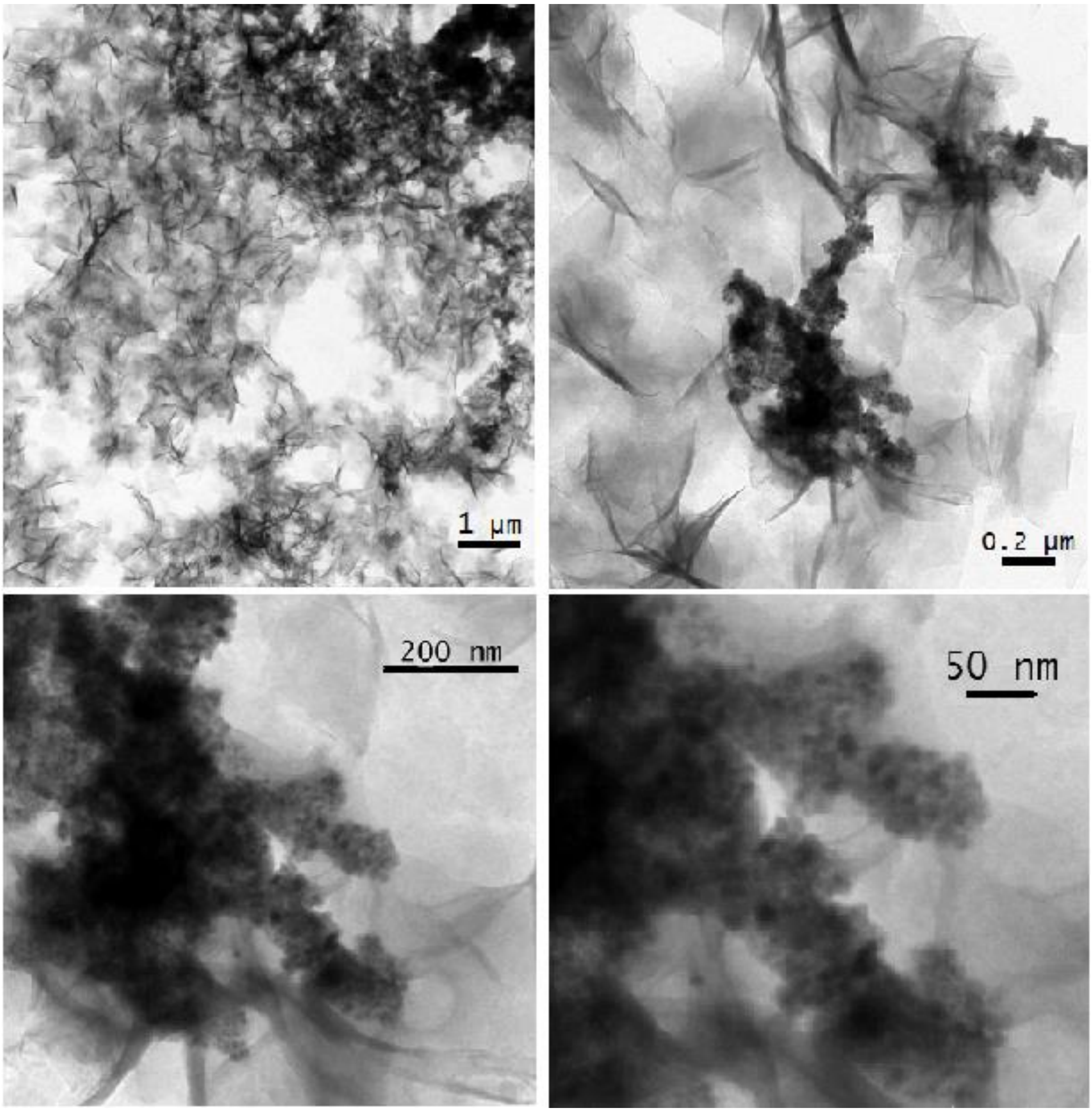

Figure S4 Bright-field TEM images at different magnifications for Ni(acac)$_2$–DEAC sample taken within the time interval **II**.

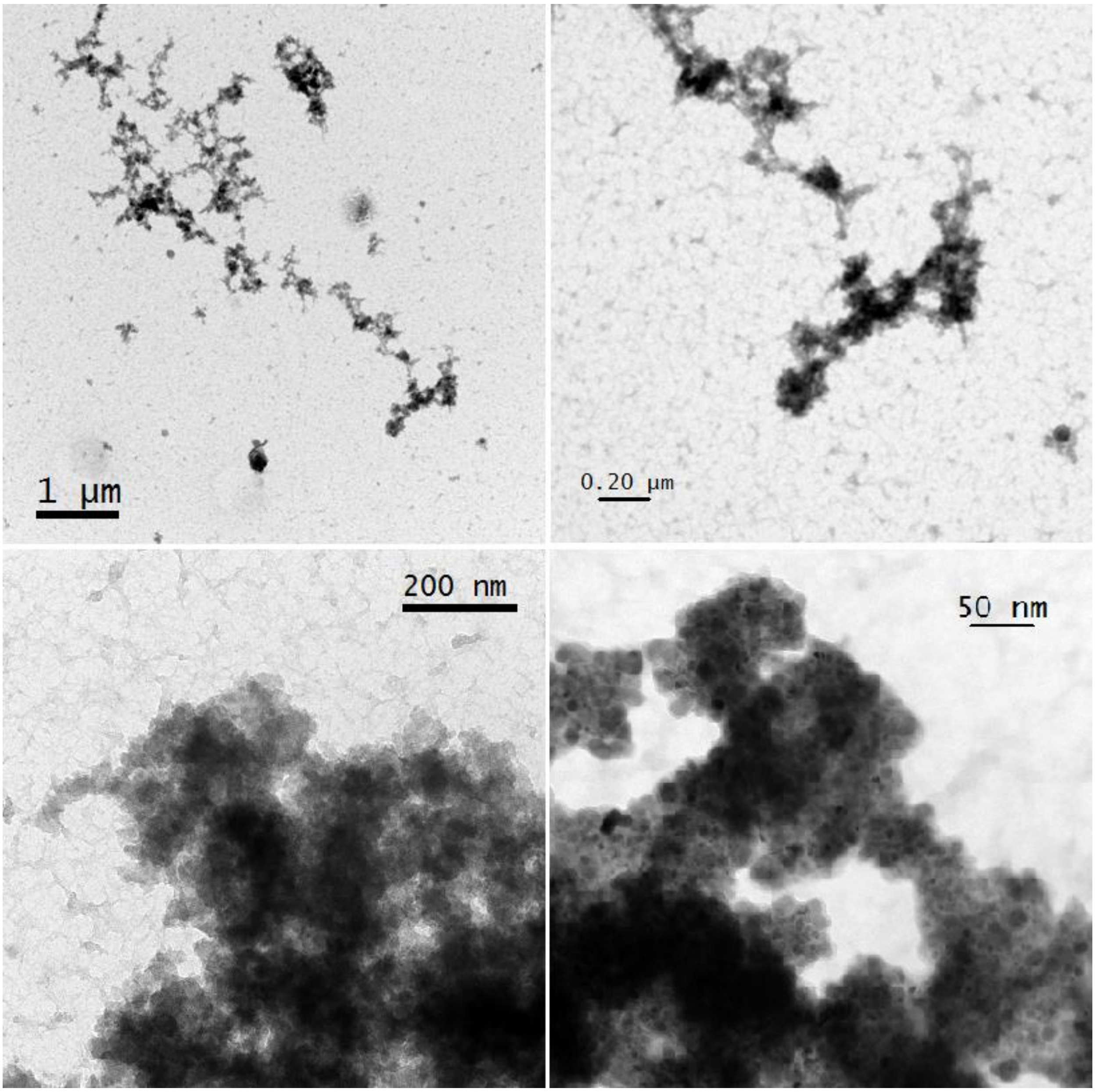

Figure S5 Bright-field TEM images at different magnifications for Ni(acac)$_2$–EASC sample taken within the time interval **II**.

The microphotographs of TEM BP for systems based on Ni(acac)$_2$–DEAC and Ni(acac)$_2$–EASC are presented in the Figure S6 and S7 (to the left), respectively. Both photographs clearly show the ordered nanoscale structures that are crystalline according to electron diffraction data. Processing of isolated sections of the photographs (secreted and marked by A, B, C, D letters) by DigitalMicrographs 3.3.1 program made it possible to obtain their profile of atomic rows (or interplanar spacings of the crystal lattice and in the literature they are often referred as d/n, Å) for each particular section (Figure S6 and S7 to the right). The digital values shown in Figure S6 and S7 and referred to in the text are additional confirmation of the data obtained on the basis of electron diffraction.

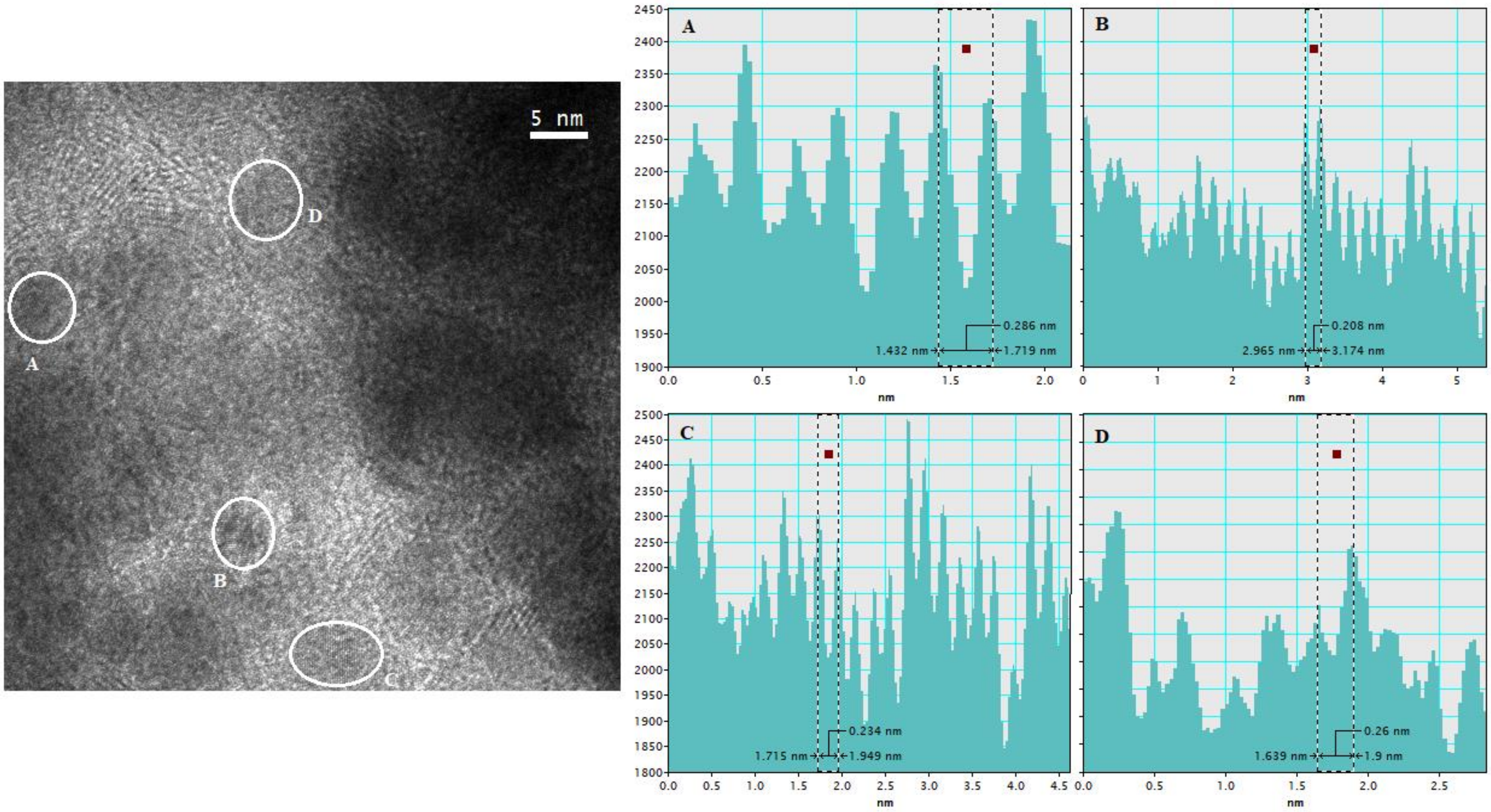

Figure S6 HRTEM image and profile of atomic rows for Ni(acac)$_2$–DEAC system.

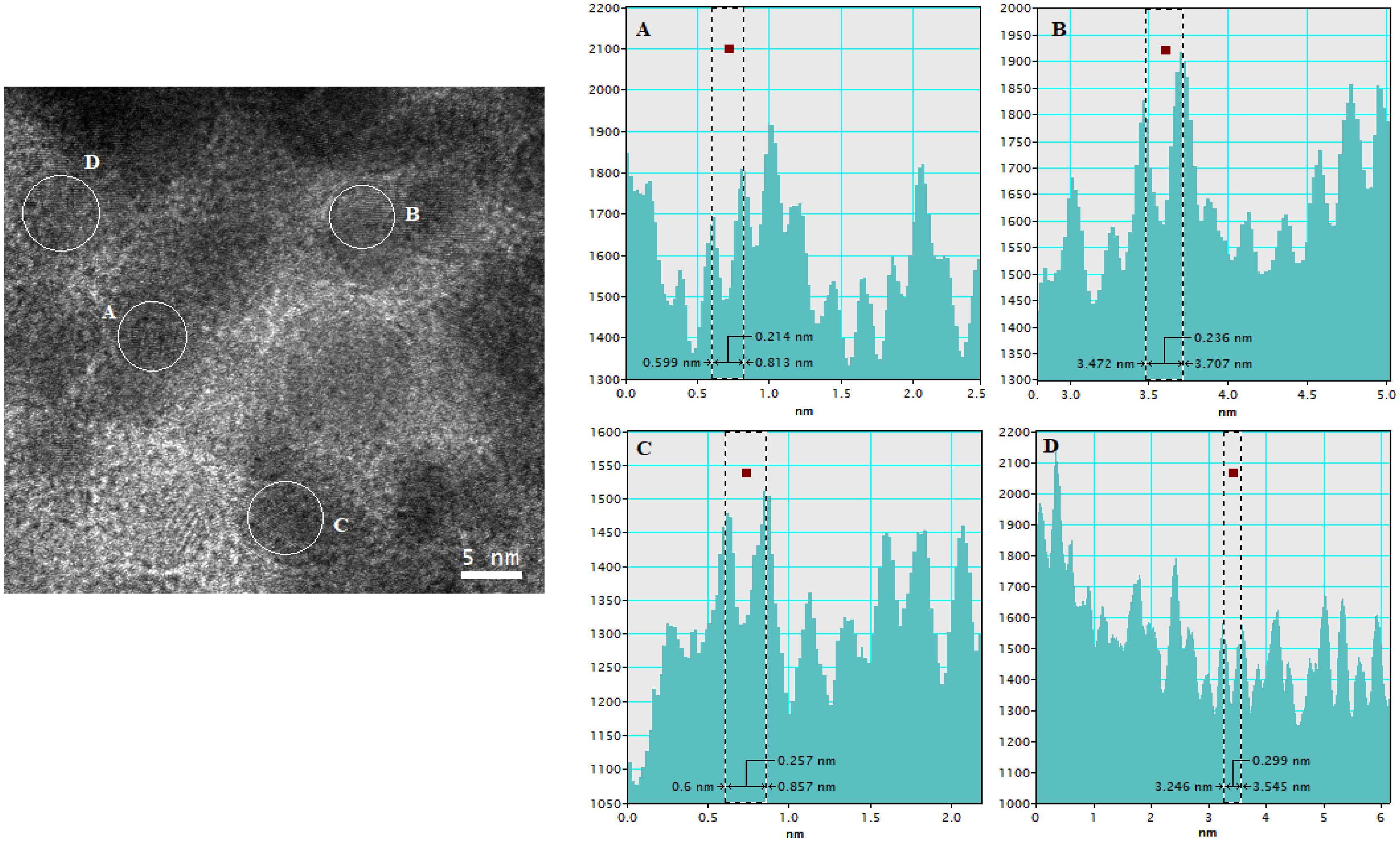

Figure S7 HRTEM image and profile of atomic rows for Ni(acac)$_2$–EASC system.

References

S1 A. J. Gordon and R. A. Ford, *The Chemist's Companion: A Handbook of Practical Data, Techniques, and References*, Wiley, New York, 1972.

S2 J. Mitchell and D. M. Smith, *Aquametry*, Wiley, New York, 1977.

S3 F. K. Shmidt, Yu. Yu. Titova and L. B. Belykh, *Kinet. Catal*., 2016, **57**, 61 (*Kinet. Katal*., 2016, **57**, 63).

S4 T. Mole and E. A. Jeffery, *Organoaluminium Compounds*, Elsevier, New York, 1972.

S5 F. K. Schmidt, Yu. Yu. Titova, S. S. Kolesnikov and L. B. Belykh, *Appl. Catal., A*, 2015, **499**, 177.

S6 M. Goswami, A. Chirila and C. Rebreyend, *Top. Catal*., 2015, **58**, 719.

S7 S. Stoll and A. Schweiger, *J. Magn. Reson*., 2006, **178**, 42.

S8 Yu. Yu. Titova and F. K. Shmidt, *Kinet. Catal*., 2017, **58**, 749 (*Kinet Katal*., 2017, **58**, 735).

S9 G. R. Eaton, S. S. Eaton, D. P. Barr and R. T. Weber, *Quantitative ESR*, Springer-Verlag, Wien, 2010.

S10 D. R. G. Mitchell, *Microsc. Res. Tech*., 2008, **71**, 588.

S11 H. Flanders, *Calculus: A Lab Course with MicroCalc*, Springer-Verlag, New York, 1996.

S12 K. H. Liland, E.-O. Rukke, E. F. Olsen and T. Isaksson, *Chemom. Intell. Lab. Syst*., 2011, **109**, 51.